A Meta-heuristic approach for Reliability-Based Design Optimization of Shell-and-Tube Heat Exchangers

Jafar Jafari-Asl [1, *], Oscar D. Lara Montaño [2], Seyedali Mirjalili [3, 4], Matthias G.R. Faes [5]

[1] INEGI & CONSTRUCT, Faculty of Engineering, University of Porto, 4200-465 Porto, Portugal.

[2] Faculty of Engineering, Autonomous University of Querétaro, Campus Amazcala, El Marqués, Querétaro, 76265, México

[3] Centre of Artificial Intelligence Research and Optimisation, Torrens University, Brisbane, Australia.

[4] University Research and Innovation Center, Obuda University, 1034 Budapest, Hungary.

[5] Chair for Reliability Engineering, TU Dortmund University, Leonhard-Euler-Straße 5, 44227 Dortmund, Germany.

[*]Corresponding author: jafar.jafariasl@yahoo.com

Abstract

This study introduces a new framework for optimizing Shell-and-Tube Heat Exchanger (STHE) layouts using a reliability-based design optimization (RBDO) approach. The framework combines a control variate-based surrogate model and a hybrid metaheuristic algorithm. The proposed hybrid algorithm, k-means clustering and whale optimization algorithm (kWOA), was evaluated using CEC'2020 and a case study for optimizing STHE design under static conditions. kWOA showed superior performance in minimizing STHE's total annual cost and solving benchmark functions effectively. In our case study, the RBDO framework optimized the STHE design under two scenarios with target failure probabilities of 1% and 5%, resulting in cost increases of 112% and 82%, respectively, compared to deterministic optimization (DO). The integration of the RBDO approach with the STHE mathematical model, considering factors like inlet flow temperatures, mass flow rates, and fouling resistance, demonstrated the framework's ability to balance the trade-off between cost and reliability under uncertainty. Hybrid control variate radial basis function (RBF) models and Monte Carlo Simulation (MCS) were used to assess safety levels, showing the RBDO framework's superiority in improving safety and significantly reducing failure probability from 89% to 1% and 5%. The RBDO framework offers a robust approach for designing STHEs that achieve optimal performance while ensuring high reliability under uncertain conditions.

Keywords: Shell-and-tube heat exchangers (STHE); Reliability-based design optimization (RBDO); Whale optimization algorithm (WOA); Uncertainty conditions; Control variate radial basis function (RBF).

1. Introduction

Heat exchangers are crucial in almost every industrial process. Their primary purpose is to recover energy and provide cooling and heating duties for process streams. Among the different available heat exchange technologies, the shell-and-tube heat exchanger (STHE) is the most widely used for industrial applications [1]. This success is a result of the fact that STHEs can operate in a wide range of temperatures and pressures, provide a good heat transfer area-to-volume ratio, and have standardized design and building procedures [2].

Concerning their design; Kern's method and the Bell-Delaware method are the two main design approaches employed to predict the thermo-hydraulic performance of STHEs. The first method considers the flow of a single stream that moves in a zig-zag pattern inside the shell side; the second methodology divides the flow into different sub-streams [2]. An illustrative representation of a STHE is shown in Fig. 1. Some common objective functions employed in the mono-objective minimization of STHE are the heat transfer area, total annual cost, area and volume footprint, and exchanger effectiveness [3]. Both design methodologies involve non-linear, non-continuous, and non-differentiable equations; furthermore, they depend on a combination of continuous and discrete design variables. This complicates the application of algorithmic design optimization procedures. Indeed, due to the non-convexity and mixed-integer nature of the optimization problem, metaheuristic algorithms are arguably the most appropriate class of methods for finding the optimal STHE design.

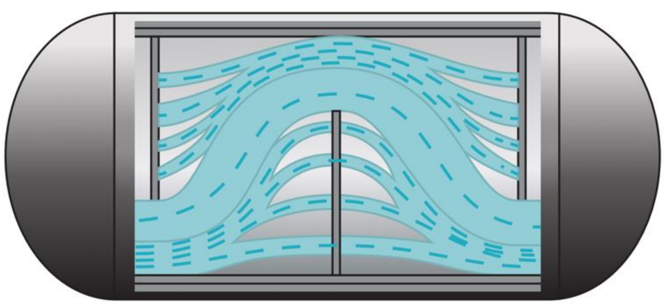

Fig. 1. Representation of the sub-streams produced in shell-side, considered in Bell-Delaware method.

1.1. Literature review

Optimization is a procedure that allows finding the best solution according to one or multiple criteria employing the least possible resources. In industry, it is possible that process equipment with different operative and geometrical characteristics can perform the same task. STHEs are not an exemption in this context. As a result, the design of this equipment can be optimized according to multiple objective functions. Caputo et al. (2022) compared various objective functions for the optimization of STHE. They point out that the best option, regarding costs and performance of STHEs is the utilization of a total cost-based objective function because it considers minimizing the heat transfer area and reducing the pressure loss. The works reported in this literature review only include cost-related objective functions [3].

The optimization process of STHEs was originally proposed with a trial-and-error procedure [1]. Later, researchers started to apply deterministic and metaheuristic optimization methods to obtain the best designs automatically. Mizutani et al. proposed an optimization model for the design of STHEs based on generalized disjunctive programming, and it is formulated as mixed-integer non-linear programming (MINLP). The model contains correlations from the Bell-Delaware method to estimate the heat transfer coefficient and the pressure drop in the shell side, and the total annual cost is used as the objective function [4]. Ponce-Ortega et al. [5] did a MILNP formulation for the optimal design of 1-2 STHEs employing the investment cost as optimization criteria. Onishi et al. [6] developed a MINLP model for the optimization of STHEs using the Bell-Delaware method, following TEMA standards rigorously. A sequential optimization approach of partial objective targets is proposed as a strategy to solve the optimization problem. It is noticeable that a deterministic method is simple and fast because it starts with a solution and moves it toward an optimum. However, the initial solution greatly affects the quality of the final solution, and there is a high chance of getting stuck in local optima. These are sub-optimal solutions that look like the best ones in a search space, but they are not. The problem is that we do not know how many times we need to run the optimizer with different initial solutions to find the best one.

Due to the high non-linearity and mixed-integer nature of the optimization problem of the design of STHEs, metaheuristic optimization algorithms have been employed. These algorithms are gradient-free methods that use stochastic variables in their structure to escape from local optima [7], maintaining a balance between exploration and exploitation. Exploration refers to the ability to generate candidate solutions in various regions of the search space, while exploitation is the capacity to obtain a high-quality solution in a specific region [8]. Metaheuristic algorithms can be categorized into four groups: evolution-based, swarm intelligence-based, physics-based, and human-related [9]. Various algorithms from each category, including Genetic Algorithm [5,10–12][5,10–12], Differential Evolution [13,14], and several physics-based optimization algorithms [15], have been used to optimize the design of STHEs.

Building on this foundation, the multi-objective optimization of heat exchangers has also been explored. Nascimento et al. utilized a Random Vector Functional Link (RVFL) network and the Non-Dominated Sorting Genetic Algorithm III (NSGA-III) for the design of plate-fin heat exchangers, focusing on maximizing effectiveness while minimizing volume and pressure drop [16]. Colaço et al. [17] employed the Non-dominated Sorting Genetic Algorithm with Reinforcement Learning (NSGA-RL), NSGA-II, and Constrained Non-dominated Sorting Genetic Algorithm (CNSGA) algorithms to optimize double-pipe heat exchangers with perforated baffles, aiming to maximize the thermal performance index (TPI) and Nusselt number while minimizing the Fanning friction factor. Hamed et al. [18] applied genetic algorithms to optimize a three-fluid heat exchanger, seeking to minimize entropy generation and maximize effectiveness. Table 1 collects some studies where different metaheuristic algorithms were applied to optimize the design of STHEs according to one or multiple objectives. It shows the algorithm(s) used and the main result.

Table 1. Review of studies on the optimization of STHEs using metaheuristic techniques.

Author	Algorithm	Objective function	Results
Sadeghzadeh et al. [10]	PSO	Total cost[1]	Compared to GA, PSO was a more effective option for two investigated case studies.
Lara-Montaño et al. [19]	GWO, PSO	Total anual cost[2]	The study created a virtual environment that can improve the heat transfer and fluid flow of STHE. The optimization methods thier used reached the vicinity of the best solutions.
Hajabdollahi et al. [20]	NSGA-II	Total cost, exergy efficiency	The study determined the design variables that had the most impact.

			Moreover, the study used GAs to perform multi-objective optimization and enhance the STHE performance.
Lara-Montaño et al. [21]	DE, GA, PSO, CS, WOA, TLBO, UMDA	Total annual cost	A comparison of the performance of different optimization algorithms to solve the optimization problem of designing an STHE with the minimum total annual cost is presented. They found that PSO can converge in the region of the best solution in a limited number of experiments.
Şencan Şahin et al. [22]	ABC	Total annual cost	The total cost is significantly lower when compared with conventional methods that rely on trial and error.
Asadi et al. [23]	CSA	Total annual cost	Its implementation generates a reduction of 77% and 48% for operation cost compared to PSO and GAs, respectively.
Nascimento et al. [16]	RVFL network, NSGA-III	Maximize effectiveness, minimize volume and pressure drop	Enhanced thermal performance in PFHE design with reduced processing time
Colaço et al. [17]	NSGA-RL, NSGA-II, CNSGA	Maximize TPI and Nusselt number, minimize Fanning friction factor	NSGA-RL outperforms in TPI improvement and non-dominated solutions
Hamed et al. [18]	Genetic algorithms	Minimize entropy generation, maximize effectiveness	Optimal mass flow rates for three streams to maximize effectiveness

[1] Includes the initial capital cost and the operating cost.; [2] Includes the capital cost, annual capital cost, and annual operating cost.

As is shown, the study of the optimization of the design of STHE from an economic point of view has been addressed using different metaheuristic algorithms. However, none of these works consider real operating conditions where variables such as the inlet and outlet temperatures or flow rate can vary due to other components of the processing system or environmental causes, or the case where these are inherently uncertain. As pointed out in [24], an adequate methodology to design STHEs comprehends not only to minimize or maximize the value of the objective function but also to find a reliable design with a low sensitivity due to changes or uncertainties in operating conditions.

1.2 Contribution of this work

In addressing the optimization of STHE design, the literature has primarily focused on the Bell-Delaware method to consider various substreams and thermo-hydraulic non-ideal phenomena within the shell-side. However, these studies often treat the STHE operation as static, neglecting real-world operational fluctuations. Our review indicates that few studies have explored these operational variances. This paper contributes to the existing research by presenting a composite metaheuristic optimization algorithm that not only acknowledges these variations but also targets the intricate search space associated with STHE design—a task that demands judicious algorithm selection due to its complexity.

The proposed algorithm amalgamates several strategies to outperform common methods reported in the literature, advancing the capabilities of STHE design optimization even further into the domain of reliability-based design optimization (RBDO). This work applies RBDO to STHE design, aiming for robustness against natural variations and uncertainties, which are scarcely investigated in references [24–26].

Moreover, we introduce a novel stochastic optimization framework that merges the k-means classification technique with the Whale Optimization Algorithm (WOA) [27]. This integration is tailored to improve the design process of STHEs. Notably, enhancements to the WOA algorithm have been confirmed by studies [18,28–31] to yield superior convergence and competitive results compared to other state-of-the-art algorithms. The basic WOA algorithm has been employed to optimize STHE design with poor results [21]. To enhance WOA's exploitation phase and address its limitations, our study presents a new variant termed kWOA.

Additionally, this paper proposes a hybrid radial basis function (RBF) coupled with the control variate technique and Monte Carlo Simulation (MCS) to determine the optimal design of STHEs under uncertainty, ensuring a safe and optimal design.

The paper is organized as follows: Section 2 explicates the STHE design problem and discusses the proposed optimization methods, including the hybrid WOA model for deterministic optimization and the RBDO framework. Section 3 introduces a case study illustrating the STHE design. Section 4 presents numerical and graphical results validating the robustness and efficiency of our proposed methods. Section 5 concludes the paper with a summary of our findings.

2. **Methodology**

This section outlines the methodology for modeling and optimizing STHEs. We employ the Bell-Delaware method for shell-side calculations, which accounts for various sub-streams and correction factors for different effects such as baffle configuration and leakages. The optimization problem involves minimizing the TAC subject to constraints on pressure drops, fluid velocity, and geometric ratios, with the aim of achieving an efficient and cost-effective design for STHEs.

2.1. Shell-and-tube heat exchanger modeling

The heat transfer area of a shell-and-tube heat exchanger is calculated using equation (1), where Q is the heat duty, U is the overall heat transfer coefficient, and T_{LMTD} is the logarithmic mean temperature difference. In the calculation of the global heat transfer coefficient, shown in equation (2), it is required the thermal conductivity of the material of the tube, k_w, the fouling factors for tube-side and shell-side, $R_{f,t}$ and $R_{f,s}$, respectively. Also, the convective heat transfer coefficient on the tube side, h_t, the convective heat transfer coefficient on the shell side, h_s, and the inner and outlet tube diameters d_i and d_o, respectively.

$$A = \frac{Q}{UF_t T_{LMTD}} \tag{1}$$

$$U = \frac{1}{\frac{1}{h_s} + R_{f,s} + \frac{d_o \ln\left(\frac{d_o}{d_i}\right)}{2k_w} + \frac{d_o}{d_i}\left(R_{f,t} + \frac{1}{h_t}\right)} \tag{2}$$

Equation (3) is used to estimate the length of tubes, where N_t is the total number of tubes.

$$L = \frac{A}{\pi d_o N_t} \tag{3}$$

2.2.1 Shell-side calculations

The Bell-Delaware method is employed to predict the thermo-hydraulic variables. This method considers the generation of sub-streams inside the shell. Equation (4) is used to calculate the convective heat transfer coefficient, h_s, which depends on the ideal convective heat transfer coefficient, h_{id}, that only considers the principal stream in the shell-side and five correction factors. J_c is the correction factor that accounts for the baffle configuration and considers the heat transfer in the window section. J_l is the correction factor that takes into consideration the shell-to-baffle and tube-to-baffle leakages, thereby correcting for baffle leakage effects. $\mathrm{J_b}$ is the correction factor that corrects for bundle and pass partition bypass streams. J_s is the correction factor that accounts for the baffle spacing at the inlet and outlet sections. Finally, J_r is the correction factor that corrects for adverse temperature gradient at laminar flow [2].

$$h_s = h_{id} J_c J_l J_b J_s J_r \tag{4}$$

The calculation of the ideal convective heat transfer coefficient is performed with equation (5), where Pr_s is the Prandtl number in shell-side, C_{ps} is the heat capacity, j is the Colburn factor, and $\mathrm{A_{o,cr}}$ is the crossflow area at or near the shell centerline for one crossflow section. The variable j is obtained with equation (6), where P_t is the pitch of tubes, Re_s is the Reynolds number in shell-side, and a is obtained with equation (7). The constants a_1, a_2, a_3, and a_4 depend on the layout angle and the value of the Reynolds number; the values for these constants can be found in [12].

$$h_{id} = j \frac{C_{ps} Pr_s^{-2/3}}{A_{o,cr}} \tag{5}$$

$$\mathrm{j} = a_1 \left(\frac{1.33}{P_t/d_o}\right)^a Re_s^{a_2} \tag{6}$$

$$a = \frac{a_3}{1 + 0.14 Re_s^{a4}} \tag{7}$$

The correction factor for baffle configuration is calculated with the equation (8). F_c is the fraction of the total number of tubes in the crossflow section.

$$J_c = 0.55 + 0.72 F_c \tag{8}$$

The factor that considers the leakages in the shell side is obtained employing the equation (9). The variables r_s and $\mathrm{r_m}$are computer according to equations (10) and (11), respectively. $A_{o,sb}$ and $A_{o,tb}$ are the shell-to-baffle leakage area and the tube-to-baffle leakage area, respectively.

$$J_l = 0.44(1 - r_s) + [1 - 0.44(1 - r_s)] \exp(-2.2 r_{lm}) \tag{9}$$

$$r_s = \frac{A_{o,sb}}{A_{o,sb} + A_{o,tb}} \tag{10}$$

$$r_{lm} = \frac{A_{o,sb} + A_{o,tb}}{A_{o,cr}} \tag{11}$$

The correction factor J_b is computed with equation (12), where r_b is the relation between the flow area available for bypass streams and the crossflow open area at or near the shell centerline, and N_{ss}^+ is the ratio between the number of sealing strip pairs and the number of tube rows crossed during flow through one crossflow section. $\boldsymbol{C}$ is a parameter that depends on the value of the Reynolds number [2].

$$J_b = \begin{cases} 1 & for \quad N_{ss}^+ \geq 0.5 \\ \exp\left(-Cr_b\left[1 - (2N_{ss}^+)^{1/3}\right]\right) & for \quad N_{ss}^+ < 0.5 \end{cases} \tag{12}$$

Equation (13) is used to calculate the value of the correction factor J_s. Where N_b is the number of baffles, $\mathrm{L_i^+} = \mathrm{L_{b,i}}/\mathrm{L_{b,c}}$ and $L_o^+ = L_{b,o}/L_{b,c}$. $L_{b,c}$ is the central baffle spacing, $L_{b,o}$ is the baffle spacing at the outlet region, and $L_{b,i}$ is the baffle spacing at the inlet region.

$$J_s = \frac{N_b - 1 - (L_i^+)^{(1-n)} + (L_o^+)^{(1-n)}}{N_b - 1 + L_i^+ + L_o^+} \tag{13}$$

And the last correction factor, J_r, is computed employing the equation (14), $N_{r,c}$ is the sum of the number of rows crossed during flow through one crossflow section between baffle tips and the number of effective rows in crossflow in the window section.

$$J_r = \begin{cases} 1 & for \quad Re_s \geq 100 \\ \left(\dfrac{10}{N_{r,c}}\right)^{0.18} & for \quad Re_s \leq 20 \end{cases} \tag{14}$$

To predict the value of the pressure drop in shell-side, equation (15) is used. The variables in equation (15) include $\Delta p_{b,id}$ and $\Delta p_{w,id}$, which represent the ideal pressure drop in the central section and the ideal window pressure drop, respectively. Other variables include N_b, which denotes the number of baffles, $N_{r,cw}$, which represents the number of effective tube rows in crossflow in the window section, and $N_{r,cc}$, which indicates the number of tube rows crossed during flow through one crossflow section between baffle tips. Correction factors are also taken into consideration, which include ζ_b , ζ_l and ζ_s. These factors account for tube-to-baffle and baffle-to-shell leakage, bypass flow, and for the inlet and outlet sections having different spacing from the central section. For further details on the computation of these variables, please refer to [2].

$$\Delta P_s = \left[(N_b - 1)\Delta p_{b,id}\zeta_b + N_b \Delta p_{w,id}\right]\zeta_l + 2\Delta p_{b,id}\left(1 + \frac{N_{r,cw}}{N_{r,cc}}\right)\zeta_b\zeta_s \tag{15}$$

2.2.2 Tube-side calculations

According to equation (2), it is necessary to calculate h_t to obtain the overall heat transfer coefficient. The calculation of $h_t$depends on the value of the Reynolds number in tube-side, Re_t. If $Re_t < 2300$ the equation (16) is employed. If $Re_t \geq 2300$ and $Re_t < 10{,}000$, the equation (17) is used. For greater values of Re_s, the heat transfer coefficient on tube-side is computed with equation (18). f_t is the Darcy friction factor.

$$\mathrm{h_t} = \frac{\mathrm{k_t}}{\mathrm{d_i}}\left[1.86\left(\frac{Re_t Pr_t d_i}{L}\right)^{(1/3)}\right] \tag{16}$$

$$h_t = \frac{k_t}{d_i}\left[\frac{\frac{f_t}{2} Re_t Pr_t}{1.07 + 12.7\left(\frac{f_t}{2}\right)^{0.5}\left(Pr_t^{2/3} - 1\right)}\right] \tag{17}$$

$$h_t = \frac{k_t}{d_i} Re_t^{0.8} Pr_t^{1/3}\left(\frac{\mu_t}{\mu_w}\right)^{0.14} \tag{18}$$

The pressure drop in tube side is obtained with equation (19). Where ρ_t is the density of the fluid, v_t is the velocity of the fluid in the tubes, N_p is the number of tube passes [1].

$$\Delta P_t = \frac{\rho_t v_t^2}{2}\left(\frac{L}{d_i} f_t + 4\right) N_p \tag{19}$$

2.2.3 Total annual cost estimation

The total annual cost (TAC) is employed as the objective function, it consists of the sum of the annualized cost of the equipment, C_c, and the operating cost, C_{op}. The annualized cost of the equipment depends on the heat transfer area and is obtained with equation (20). C_M, C_P and C_T are factors whose value depends on the construction material, operating pressure, and operating temperature, respectively. r is the interest rate, and n is the projected lifetime. The interest rate is 5%, and the projected lifetime 20 years. Also, the values for C_M, C_P and C_T are 1.7, 1.0, and 1.0.

$$\mathrm{C_c} = \left(3.28\mathrm{e}4 \left(\frac{A}{80}\right)^{0.68} C_M C_P C_P\right) \frac{\mathrm{r}(1+\mathrm{r})^n}{(1+r)^n - 1} \tag{20}$$

Equation (21) is used to calculate the operating cost. It depends on the pumping powers required in hot and cold sides. E_s and E_t are the pumping power in the shell-side and tube-side, respectively. E_c is the cost of energy, and H_r is the number of working hours per year. The cost of electricity is taken as 0.1 USD/kWh and the pumping efficiency is 0.85.

$$\mathrm{C_{op}} = \frac{(\mathrm{E_s} + \mathrm{E_t})\mathrm{E_c}\mathrm{H_r}}{1000} \tag{21}$$

2.2.4 Optimization problem

As mentioned, the objective function is the TAC that must be minimized. The optimization problem depends on eleven decision variables. Seven decision variables are continuous, and four are discrete. A range of valid values is given for each continuous decision variable; this is shown in Table 2. The allowed values for discrete decision variables are given in Table 3.

Table 2. Range of valid values for continuous decision variables.

Design variable		Lower bound	Upper bound
Diameter of shell	D_s	300 mm	1,500 mm
Outer diameter of tube	d_o	6.35 mm	50.8 mm
Baffle spacing at center	L_{bc}	$0.2D_s$	$0.55D_s$
Baffle spacing at the center	L_{bo}, L_{bi}	L_{bc}	$1.6L_{bc}$
Baffle spacing at the inlet and outlet	δ_{tb}	$0.01d_o$	$0.1d_o$
Diametrical clearance of shell-to-baffle	δ_{sb}	$0.01D_s$	$0.1D_s$
Outer diameter of tube bundle	D_{otl}	$0.8(D_s - \delta_{sb})$	$0.95(D_s - \delta_{sb})$

Table 3. Allowed values for discrete decision variables.

Design variable		Allowed values
Tube pitch	P_t	$[1.25d_o, 1.5d_o]$
Tube layout angle	TL	$[30º, 45º, 90º]$
Baffle cut	B_c	[25%, 30%, 40%, 45%]
Number of tube passes	B_c	$[1, 2, 3]$

Additionally, some geometric and operative constraints are applied. These are shown in equations (22)-(24). The pressure drop on both sides must be smaller than 70,000 Pa, the fluid velocity on tube-side must be between 0.5 m/s and 1.5 m/s, and the ratio between the length of the tubes and the internal diameter of the shell must be lower than 15. If a constraint is violated, the value of the objective function is penalized.

$$\Delta P_s, \Delta P_t \leq 70{,}000\ Pa \tag{22}$$

$$0.5\ m/s\ \leq v_t \leq 3\ m/s \tag{23}$$

$$L/D_s < 15 \tag{24}$$

The optimization problem is shown in equation (25), it consists of one objective function to minimize, five geometric and operative constraints, and a set of constraints for each decision variable. dv is referred to the i decision variable, lb and ub are vectors that contain the lower and upper admissible values for the decision variables, respectively.

$$\begin{aligned} \min_{\mathrm{x}} \quad & TAC(x) \\ s.t. \quad & \Delta P_s \leq 70{,}000\ Pa \\ & \Delta P_t \leq 70{,}000\ Pa \\ & v_t \geq 0.5 \\ & v_t \geq 3 \\ & L/D_s < 15 \\ & dv_i > lb_i \\ & dv_i < lb_i \end{aligned} \tag{25}$$

2.2 Proposed k-means-based algorithm

In this section, we introduce a novel k-means-based algorithm that combines the WOA with k-means clustering to enhance the optimization process for STHEs. The WOA, inspired by the hunting behavior of killer whales, employs mechanisms such as encircling prey, spiral bubble-net feeding maneuvers, and searching for prey to update candidate solutions. To address the limitations of WOA, such as its low exploitation ability and potential to get stuck at local optima, we integrate the k-means clustering algorithm. This algorithm divides the population of search agents into clusters, allowing for more focused exploration and exploitation within the design space.

2.2.1. Whale optimization algorithm

The WOA was developed by Mirjalili and Lewis in [27]. This optimization algorithm emulates the hunting of killer whales that consists of encircling the prey, spiral bubble-net feeding maneuvers, and searching for the prey.

As with most metaheuristic optimization algorithms, the WOA starts generating random candidate solutions within the imposed limits for the design variables. According to the source of inspiration for this optimization algorithm, each candidate solution is represented by a whale, and the prey is the optimum solution. The first phase employed to update the solutions consists of encircling the prey. In nature, humpback whales can identify the position of their prey; however, it is impossible to know *a priori* the values of the elements of the solution vector. The WOA assumes that the current best candidate solution is the target prey or at least that it is close to the optimum. Once the best current candidate solution is identified, the other search agents update their positions according to equations (26) and (27). Where t is referred to the current iteration, $\vec{A}$, and $\vec{C}$ are vectors of coefficients, $\vec{X}^*$ is the vector for the current best candidate solution of the iteration t, $\vec{X}$ is a vector of each candidate solution, | | represents the absolute value, and · is the operator for element-by-element multiplication.

$$\vec{D} = \left|\overrightarrow{C} \cdot \overrightarrow{X^*}(t) - \vec{X}(t)\right| \tag{26}$$

$$\vec{X}(t+1) = \vec{X}^*(t) - \vec{A}\vec{D} \tag{27}$$

The vectors of coefficients $\vec{A}$ and $\vec{C}$ are calculated according to the equations (28) and (29). Where a a parameter that linearly decreases from 2 to 0 in the iterative process, and $\vec{r}$ is a vector whose elements are random numbers from 0 to 1. As a decreases in the iterative process, the transition from exploration to exploitation takes place.

$$\vec{A} = 2\vec{a} \cdot \vec{r} - \vec{a} \tag{28}$$

$$\vec{C} = 2 \cdot \vec{r} \tag{29}$$

WOA was developed to perform the exploration and exploitation phases employing different operators. The designers of this optimization algorithm named the exploitation phase the bubble-net attacking method and the exploration phase the *search for prey*. The *bubble-net attack method* consists of (i) the *shrinking encircling mechanism* that is obtained by the decrementing of the parameter a from 2 to 0 in equation (28), and (ii) the *spiral updating position* where equation (30) is employed to mimic the helix-shaped movement of humpback whales. Equation (31) indicates the distance between the prey and a candidate solution, b is a constant used to define the shape of the spiral, and l is a random number between -1 and 1.

$$\vec{X}(t+1) = \overrightarrow{D'} \cdot e^{bl} \cdot cos(2\pi l) + \vec{X}^*(t) \tag{30}$$

$$\overrightarrow{D'} = |\vec{X}^*(t) \;-\; \vec{X}(t)| \tag{31}$$

Humpback whales use both patterns to swim around the prey. To model this behavior, it is assumed that in the updating process, equations (27) and (30) have the same probability to be chosen.

The *search for prey* mechanism occurs when the $|A| \geq 1$; this occurs in the first half of the iterative process has passed. Furthermore, equations (32) and (33) are used to enhance the search space exploration to update the candidate solutions. A random solution, $\overrightarrow{X_{rand}}$ is selected from the current population of candidate solutions.

$$\vec{D} = \left|\vec{C} \cdot \overrightarrow{X_{rand}} - \vec{X}\right| \tag{32}$$

$$\vec{X}(t+1) = \overrightarrow{X_{rand}} - \vec{A} \cdot \vec{D} \tag{33}$$

The equations that influence the updating mechanism through the iterative process are selected depending on the value of A. If $|A| < 1$, the candidate solutions are updated according to the *bubble-net attack method*; otherwise, the *search for prey* mechanism is applied.

As previously stated, the WOA has a superior ability to explore the design space and find promising solutions. However, the WOA also has some limitations, which are outlined below:

- However, the WOA may have low exploitation ability, which can result in solutions with low accuracy for the challenging, high-dimensional optimization problem.
- Additionally, while WOA is effective in avoiding local optima and has good global search capability, it can still get stuck at local optima.
- The three social behavior models used in WOA may create an imbalance between the exploration and exploitation stages, leading to decreased solution accuracy.

Nonetheless, the WOA has increased researchers' interest in solving challenging, high-dimensional optimization problems [28–34]. To further improve its performance and efficiency in solving real-world problems, particularly the design problem of STHEs, the main motivation of the study is to integrate a clustering algorithm, with the WOA.

2.2.2. K-means clustering algorithm

In addition to the importance of optimization techniques, data analysis is an important area for researchers to explore. One of these techniques is clustering, which provides insight into the underlying structure of the data. The k-means technique is one of the most popular clustering algorithms. It was first introduced in [35]. The main task of the k-means algorithm is to divide data into subgroups based on a distance metric between points from together. The main steps of the k-means algorithm are outlined below:

- The first step is defining the number of subgroups, followed by randomly selecting their centroids.
- Then, the Euclidean distance between the points and the centers is calculated, and the points are grouped based on their nearest center. New centers are then determined based on the groupings.
- The process of changing the centers of the groups continues until their positions are fixed.

A squared error function that serves as the objective function, shown in equation (34), is minimized during this process.

$$J\sum_{i=1}^{c}\sum_{j=1}^{ci}||||x_i^j - c_j||\,||^2 \tag{34}$$

In which, $||x_i^j - c_j||$ represents the Euclidean distance between two points x_i and c_j. x_i and c_j are the number of data points and cluster centers.

2.2.3. K-means based whale optimization algorithm

The hybrid algorithm proposed in this study is based on the main idea presented in [36], in which the performance of GWO was improved. In the k-means-based WOA, after initializing the first population of search agents. The population is divided into two clusters using the K-means algorithm, after which the fitness of solutions is computed for each cluster separately. Once the population is classified into two clusters, a condition is introduced that depends on a random number between 0 and 1. If the random value is greater than 0.5, the algorithm operates on the population clusters based on their fitness. Within this condition, the fitness values of both clusters are compared, and if the fitness of cluster 1 is lower than that of cluster 2, the search agents' position is set to cluster position 1 and vice versa. However, if the random number is less than or equal to 0.5, the algorithm operates on the original population without clustering.

2.2.4. Reliability-based design optimization approach

The RBDO problem is commonly defined as an optimization problem with dynamic probabilistic constraints, which can be expressed as shown in expression (35) [26,37]:

$$\begin{aligned} &\text{Minimize } \ f\,(\boldsymbol{d}) \\ &\text{Subject to } \ P_{f,i}[G_i(\boldsymbol{X},\boldsymbol{d}) \le 0] \le P_{f,i}^{t}\,, i = 1, \dots, N \\ &\qquad\qquad \boldsymbol{d}^l \le \boldsymbol{d} \le \boldsymbol{d}^u \end{aligned} \tag{35}$$

where $\boldsymbol{X}$= $\{\boldsymbol{X}_{,i}\}_{i=1}^{m}$and $\boldsymbol{d}$= $\{\boldsymbol{d}_i\}_{i=1}^{n}$ represent the vectors of random and design variables, respectively. f is the objective function (e.g., mass, volume, and cost), $\{G_i\}_{i=1}^{N}$ and $\{P_{f,i}\}_{i=1}^{N}$are the limit state function (LSF) of the *i*-th probabilistic constraint and the corresponding failure probability, respectively. In the equation, $\{P_{f,i}^{t}\}_{i=1}^{N}$ represents the desired failure probability of the *i*-th probabilistic constraint, while $\boldsymbol{d}^l$ and $\boldsymbol{d}^u$ represent the lower and upper bounds of the design variables, respectively. The failure probability of each constraint is calculated through the integral of the equation (36). Where f_X denotes the joint probability density function of $\boldsymbol{X}$ [37].

$$P_f = \int_{G(\boldsymbol{X})\le 0} f_{\boldsymbol{X}}(x)dx \tag{36}$$

Since calculating the failure probability of each constraint may require a significant number of evaluations of the LSF, finding the optimal design for this complex problem can be challenging. To address this challenge, a control-variate-based surrogate method is integrated into the framework to estimate the effect of uncertainties on parameters in the RBDO process and the response of STHE. To build the surrogate model and predict the design's performance based on design points, the radial basis function (RBF) [38] is utilized. The RBF is a form of artificial neural network (ANN) that comprises input, hidden, and output layers. In this model, the input layer is responsible for transferring data to the hidden layer, which is the second layer. The hidden layer is composed of numerous neurons, each of which employs a specific algorithm in two stages. In the first stage, the square roots of the inputs of the hidden layer are computed using their weights and the Euclidean function. In the second stage, a Gaussian activation function is applied to the output of the first stage. This can be mathematically expressed as equation (37) shows:

$$q_i = g_i(\|X - C_i\|) = \exp(-\frac{\|X - C_i\|^2}{2{\sigma_i}^2}) \quad (37)$$

In which the X represents the vector of variables; here, g_i(X)= g_i(||X - C_i||) represents the Gaussian activation function, C_i represents the center of the activation function, ||*|| represents the Euclidean nor//m, and σ_i represents the width of the receptive field for the RBF. Equation (38) can be utilized to represent the activation of the output layer, which is the result of a linear combination of the units within the hidden layer:

$$y = \sum_{i=1}^{n} w_i\, q_i \quad (38)$$

Here, w_i represents the connecting weights from the hidden layer to the output layer.

There are several techniques for designing the RBFN. The optimization algorithm introduced in this study was utilized for the purpose of training and designing the neural network. This approach involves utilizing each input data point as the center of the activation function for a hidden node. The weights of the second layer are then determined by solving an optimization problem, with considering the minimization the network error as an objective function [39]. It is important to mention that the training process of the network continues until the network error is reduced to zero.

The process of evaluating the accuracy of predicted responses involves calculating the absolute percentage error (APE), mean absolute percentage error (MAPE) between the predicted and actual responses, as well as the standard deviation (SD) of APEs (Eqs 39-41) [40]

$$APE_i = 100\left|\frac{\lambda^i_{actual} - \lambda^i_{predicted}}{\lambda^i_{actual}}\right| \quad (39)$$

$$MAPE = \frac{1}{n}\sum_{i=1}^{n}(APE_i) \quad (40)$$

$$SD = \sqrt{\frac{1}{n-1}\sum_{i=1}^{n}(APE_i - MAPE)^2} \quad (41)$$

In which, n is the number of samples. Once the surrogate model is constructed in the RBDO process based on the responses of the support points by the RBF, the probability of failure is calculated through equation (42).

$$\widehat{P}_f = \int_{\mathbb{X}} \pi_{\hat{g} \leq 0}(x) f_X(x) dX, \tag{42}$$

where $\hat{g}$ is the surrogate (estimated) function and $\pi_{\hat{g} \leq 0}$ is the index function that is calculated by equation (43) [41].

$$\pi_{\hat{g} \leq 0}(x) = \begin{cases} 0 & \hat{g}(x) \leq 0 \\ 1 & \hat{g}(x) > 0 \end{cases} \tag{43}$$

Surrogate-based models are the cost-effective alternative techniques to other common reliability methods and can reasonably approximate the limit-state function (LSF). However, they may not be sufficient when it comes to estimating the original LSF ($g(x) \neq \hat{g}(x)$) in nonlinear/complex problems [41,42]. Several attempts have been made to address the errors of alternative methods. Rashki et al. [41] proposed a control variable approach to eliminate the estimation error of surrogate models. They demonstrated the effectiveness of this approach using kriging and response surface methods to solve the reliability assessment problem of STHEs. Based on their findings, they recommended the use of the control variable (CV) method to correct the estimation error of the LSF in surrogate models for other regression methods.

Therefore, the current study employs the CV technique to modify the calculated failure probability value and eliminate the prediction error of the LSF when using the RBF in RBDO process. By employing a CV technique and surrogate model, an accurate estimation of failure probability is refined as follow:

$$P_f = \alpha . \widehat{P}_f \tag{44}$$

where is α the regression coefficient of CV technique and can be calculated with equation (45).

$$\alpha\ (xDoE) = \frac{\sum_{i=1}^{N_{cor}} \left(\mathbb{I}_{g(X) \leq 0}\left(x_{DoE}^{(i)}\right) . \frac{f_X\left(x_{DoE}^{(i)}\right)}{h^*\left(x_{DoE}^{(i)}\right)} \right)}{\sum_{i=1}^{N_{cor}} \left(\pi_{\hat{g}(X) \leq 0}\left(x_{DoE}^{(i)}\right) . \frac{f_X\left(x_{DoE}^{(i)}\right)}{h^*\left(x_{DoE}^{(i)}\right)} \right)} \tag{45}$$

where h^* is a sampling function that is utilized to generate the samples of support points based on the function $f_{(X)}$. Also, $xDoE$ refers to the support points generated for constructing the surrogate RBF model.

The proposed approach eliminates the drawbacks of RBF during reliability analysis and further improves the failure probability through classification correction [37].

The proposed metaheuristic-based framework for reliability-based design optimization of SHTEs consists of two main parts: the first part utilizes the k-means clustering technique to improve the performance of the WOA algorithm for the optimization of SHTEs; the second part uses a hybrid control variate-based surrogate model to handle the probabilistic constraints of the problem. Fig. 2 presents the flowchart of the proposed framework. Algorithm 1 outlines the kWOA pseudo code to solve the RBDO problem of STHEs, while the detailed explanations are presented as follows:

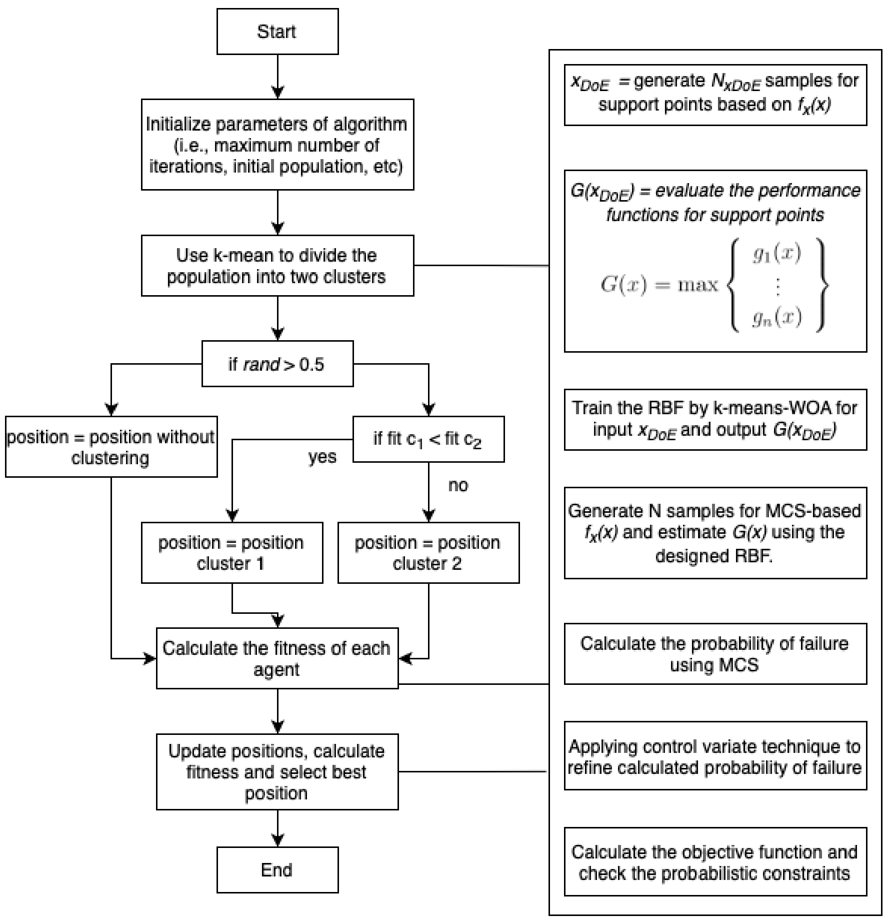

Fig. 2 The flowchart of framework.

Algorithm 1 Pseudo code of the proposed k-means WOA for RBDO of SHTEs.

1: **Input**: The probabilistic constraints and the information of random variable
2: Defining the SHTEs optimization problem using Eq. (25) as an RBDO problem based on Eq. (35)
3: Set the population size, the maximum number of iterations, PDF of random variables, lower and upper bounds of design variables, dimension of problem
4: Generate initial population X_i where $(i = 1, 2, 3, \ldots, n)$
5: Use K-means to divide the population
6: Calculate fitness C_1 and fitness C_2
  if $rand > 0.5$
    if $fitness\ C1 < fitness\ C2$
      $Positions = Positions\ C1$
    else
      $Positions = Positions\ C2$
    end
  else
    $Positions = Positions$
  end
7: ***while*** termination condition $(It < It_{\max})$ **do**
8: Update WOA parameter's $(i.e., a, A, C, L, and\ p)$
  if $(p < 0.5)$
    if $(|A| < 1)$
      Update the position of the current search agent by using Eq. (27)
    else if $(|A| \geq 1)$
    Select a random search agent (X_{rand})
    Update the position of the current search agent by using Eq. (30)
    end
    else if $(p \geq 0.5)$
    Update the position of the current search agent by using Eq. (33)
    end
  end
9: Check the boundary and calculate the fitness value of whales
10: Update X^* if there is a better solution $It = It + 1$
11: ***end***
12: Return X^*

The process begins with initialization, where the algorithm's parameters are set. An initial set of solutions is generated and then segmented into two distinct clusters through the k-means clustering algorithm. The fitness of each cluster is evaluated. To update the candidate solutions, a probability criterion is applied; if the probability criteria are not satisfied, this is that the random value generated is larger than 0.5, and the candidate solution is not updated. Otherwise, if the probability criteria are meet a candidate solution of each cluster are compared according to their fitness value, the candidate solution is updated with the one with the best fitness value.

Next, the focus shifts to calculating the objective function. This involves generating random variables according to the Probability Density Function (PDF) of the variables under consideration. Design points, also known as the Design of Experiments (DoE), are then selected, and the limit state functions (LSFs) are evaluated. These design points are used to train a Radial Basis Function (RBF) neural network, which is then employed to predict the system's responses for the samples generated in the previous step. The failure probability (P_f) of the system is calculated using the Monte Carlo Simulation (MCS) approach. A control variate approach is applied to refine the failure probability's accuracy.

Following this, the algorithm verifies whether the probabilistic constraints are met. Steps two and three are repeated iteratively until the termination conditions of the algorithm are fulfilled, indicating the completion of the optimization process.

3. Case study

In this particular case study, distilled water is located on the shell-side with a flow rate of 22.07 kg/s, and the inlet and outlet temperatures are 33.9◦C and 29.4◦C, respectively. Raw water is present in the tube-side with a flow rate of 35.31kg/s, and the inlet and outlet temperatures are 23.9◦C and 26.7◦C, respectively. The construction materials used in this setup are carbon steel for the shell and stainless steel for the tubes. The correction factors employed for calculating the setup cost are $C_m = 1.7$, $C_t = 1.0$, and $C_p = 1.0$. The projected lifetime period for this system is 20 years, with an interest rate of 5%, and 8000 operative working hours per year. The cost of electricity is assumed to be 0.1 USD/kWh, and the pump efficiency is estimated to be 0.85 [21].

4. Results

4.1. Evaluating the efficiency of kWOA

To confirm the efficiency of the proposed k-means-based WOA in solving the optimization problems, 10 mathematical test functions from CEC’2020 are used. Reference [43] provides the main details of the CEC’2020 test functions. The CEC’2020 series includes unimodal (f_1), multimodal (f_2-f_4), Hybrid (f_5-f_7) and composition (f_8-f_{10}) functions. To confirm the efficiency of the k-means-based WOA, we compared it with five recently proposed metaheuristic algorithms, including the Harris Hawk Optimization (HHO) [44], Generalized Normal Distribution Optimization (GNDO) [45], Ant Lion Optimizer (ALO) [46], Dragonfly Algorithm (DA) [47], and WOA [27], as well as two well-known older algorithms, Genetic Algorithm (GA) [48] and Particle Swarm Optimization (PSO) [49]. The maximum number of iterations and population number were set to 500 and 50, respectively, for all test functions. The values of parameter settings for each optimization algorithm are reported in Table 4. We use the default settings of the algorithms, as Arcuri and Fraser [50] recommend this as a fair and suitable practice. This also lowers the chance of bias due to better parameter tuning, since we do not change the default values of any algorithm.

Table 4. Parameter setting of algorithms.

Algorithms	**Parameters setting**
HHO	$E_0 \in [-1, 1], \beta = 1.5$
GNDO	-
ALO	$c_1 \in [0, 2]$
DA	$\beta = 0.5$
WOA	$a \in [0,2], A \in [0,2], L \in [-1,1], B = 1, C = 2.rand(0,1)$
GA	Crossover rate = 0.8, Mutation rate = 0.03
PSO	$c_1 = 2, c_2 = 2, \omega = 0.9$
kWOA	$a \in [0,2], A \in [0,2], L \in [-1,1], B = 1, C = 2.rand(0,1)$ Number of clusters= 2

To obtain statistical results, the selected algorithms were applied 20 times to the benchmark functions. Statistical results for CEC'2020 functions are reported in Table 5. The mean and standard deviation of the objective function calculated by the kWOA are better compared to those calculated through other metaheuristic techniques in most of the benchmark functions. The proposed algorithms generate the best values for ten of the twenty statistical variables. The GNDO algorithm obtains the second position, obtaining the best values for only four of the twenty statistical results. For example, the value of the average (1638.21) and standard deviation (1977.73) of objective function f_1 over all runs calculated through the kWOA are lower than the other techniques. The kWOA has generally outperformed other algorithms in solving the 10 benchmark problems. Specifically, it has achieved the lowest average objective function value and standard deviation from functions 1, 4, 7, and 10. Moreover, functions 8 and 9 have achieved the lowest average objective function value in 20 implementations. However, for two other functions, numbers 2 and 5, as well as the lowest standard deviation of function 9, the GNDO has achieved the lowest values, placing second overall.

Table 5. The statistical analysis of obtained results from algorithms.

Functions	Parameter	HHO	GNDO	ALO	DA	WOA	GA	PSO	kWOA
f_1	Average	1.824E+07	3.202E+03	4.083E+03	3.673E+03	4.186E+06	6.276E+06	5.049E+03	**1.638E+03**
	Std*	1.473E+07	3.210E+03	3.804E+03	2.420E+03	1.279E+06	3.285E+06	3.888E+03	**1.978E+03**
f_2	Average	3.276E+03	**1.317E+03**	2.697E+03	1.864E+03	3.239E+03	3.001E+03	1.848E+03	1.807E+03
	Std	4.852E+02	**1.466E+02**	6.067E+02	3.015E+02	5.268E+02	4.714E+02	4.148E+02	2.151E+02
f_3	Average	**7.482E+02**	7.491E+02	7.734E+02	7.632E+02	9.131E+02	8.513E+02	7.529E+02	8.479E+02
	Std	**9.060E+00**	9.800E+00	1.597E+01	1.166E+01	2.410E+01	2.893E+01	2.209E+01	2.456E+01
f_4	Average	1.924E+03	1.904E+03	1.904E+03	1.904E+03	1.925E+03	1.921E+03	1.904E+03	**1.902E+03**
	Std	9.220E+00	1.630E+00	2.880E+00	9.500E-01	6.650E+00	5.383E+00	9.409E-01	**5.700E-01**
f_5	Average	3.856E+05	**2.214E+03**	9.731E+04	2.808E+05	5.708E+05	4.070E+05	4.531E+05	1.291E+05
	Std	2.717E+05	**2.080E+02**	6.472E+04	1.854E+05	4.019E+05	2.651E+05	3.195E+05	8.611E+04
f_6	Average	2.010E+03	1.917E+03	2.011E+03	**1.624E+03**	1.745E+03	2.049E+03	1.748E+03	1.676E+03
	Std	0.000E+00	0.000E+00	0.000E+00	0.000E+00	0.000E+00	4.793E-13	2.397E-13	0.000E+00
f_7	Average	5.129E+05	8.103E+04	1.966E+04	1.310E+05	2.306E+05	4.300E+05	9.961E+04	**2.425E+03**
	Std	3.629E+05	8.532E+04	1.166E+04	1.696E+05	1.695E+05	2.730E+05	1.152E+05	**1.552E+02**
f_8	Average	2.317E+03	2.492E+03	2.457E+03	3.108E+03	3.075E+03	2.313E+03	2.866E+03	**2.302E+03**
	Std	2.460E+00	8.565E+02	6.982E+02	1.307E+03	1.340E+03	**1.343E+00**	1.193E+03	1.650E+00
f_9	Average	2.927E+03	2.824E+03	2.905E+03	2.859E+03	3.129E+03	2.924E+03	2.840E+03	**2.672E+03**
	Std	2.456E+01	**8.480E+00**	7.860E+01	2.758E+01	7.873E+01	1.901E+01	1.720E+01	1.569E+02
f_{10}	Average	2.999E+03	2.942E+03	2.951E+03	2.944E+03	2.972E+03	2.991E+03	2.945E+03	**2.913E+03**
	Std	2.932E+01	2.743E+01	3.743E+01	2.617E+01	3.064E+01	5.124E+01	2.503E+01	**3.310E+00**

* Standard deviation.

Fig. 2 displays the convergence curves generated from the selected algorithms and the kWOA. It is worth mentioning that the convergence curves presented in the figure were chosen at random from the 20 runs that were conducted. As Fig. 2 shows, the proposed optimizer has better accuracy and faster convergence than most of the optimization algorithms used in this comparison. Also, in all cases it has a better performance compared to the WOA algorithm. As given in Fig. 3, the results indicate that the k-means-based WOA can prepare a desirable equilibrium between two major phases of the algorithm (i.e., the exploration and the exploitation). Thus, it can be said that the k-means-based WOA can be beneficially used to solve a variety of optimization problems with preferable results and persuasive convergence rate.

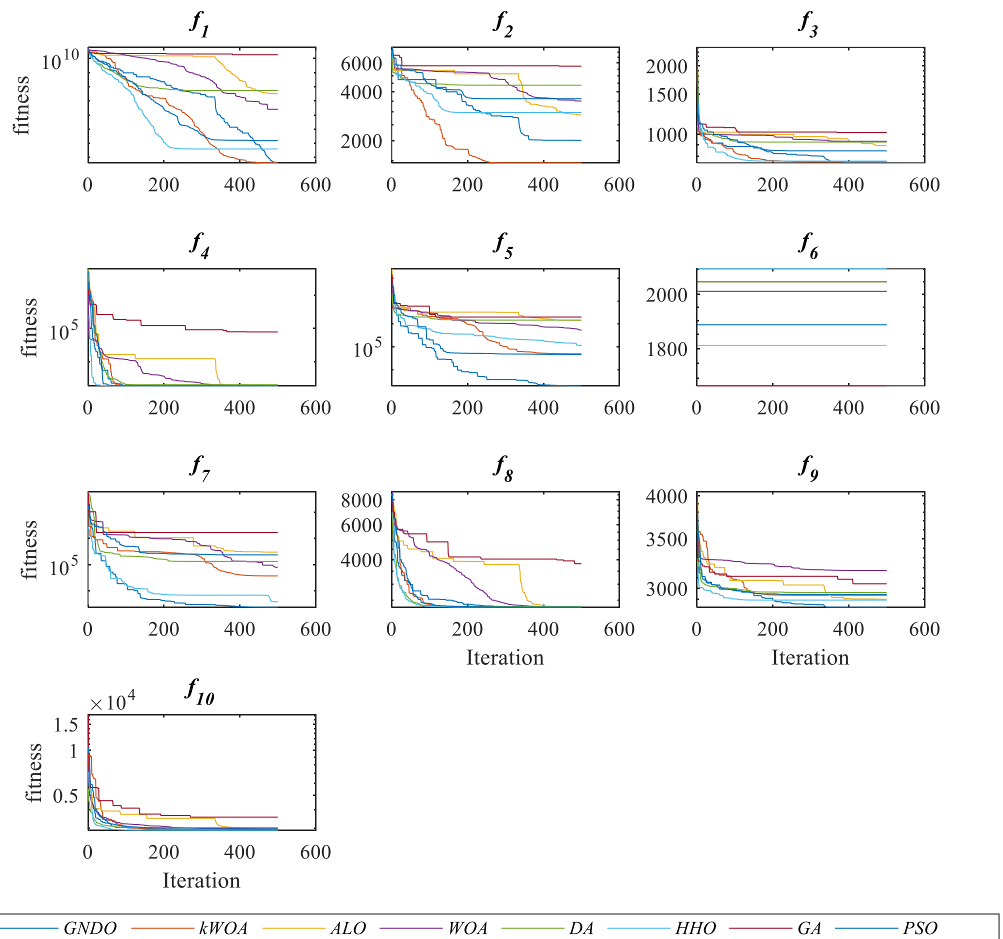

Fig. 3 The convergence curves of algorithms.

4.2. DO of STHE

In this section, a DO approach is developed to optimize the cost of design and operation of STHE using proposed kWOA, HHO, GNDO, DA, ALO and WOA on the introduced case study in section 3. To meet this aim, the simulation-optimization models with 11 design variables (i.e., D_s, d_o, L_{bc},

$L_{bo}, L_{bi}, \delta_{tb}, \delta_{sb}, D_{otl}, P_t, TL$, and B_c) were implemented. The values of the setting parameters for all algorithms were set according to Table 4 as in the previous section. Statistical parameters, including the mean, the best, worst, and standard deviation for the objective function of problems, are listed in Table 6. According to the reported results in Table 6, the kWOA can provide extremely competitive and promising solutions compared with the other algorithms. In addition, the obtained values of the best, the mean, the worst, and the standard deviation of optimization cost are 5.720E+03 USD/year, and 9.09E-13 USD/year, respectively. These values are the best compared to the generated employing the rest of the optimization algorithms. Therefore, is clear that the proposed k-means-based WOA is reliable not only for benchmark functions, but also for applications such as the design of STHEs.

Table 6. Statistical analysis of optimization results by metaheuristic algorithms.

No. runs	HHO	GNDO	ALO	DA	WOA	GA	PSO	kWOA
1	5.720E+03	5.720E+03	5.786E+03	5.913E+03	6.882E+03	6.254E+03	5.720E+03	5.720E+03
2	5.720E+03	5.721E+03	5.720E+03	5.913E+03	7.492E+03	6.242E+03	5.911E+03	5.720E+03
3	5.721E+03	5.720E+03	5.720E+03	5.910E+03	7.552E+03	5.720E+03	6.004E+03	5.720E+03
4	5.720E+03	5.720E+03	5.720E+03	5.910E+03	6.162E+03	6.805E+03	5.866E+03	5.720E+03
5	5.720E+03	5.889E+03	5.720E+03	5.930E+03	8.186E+03	5.841E+03	5.796E+03	5.720E+03
6	5.721E+03	5.817E+03	5.720E+03	6.075E+03	7.409E+03	5.882E+03	5.720E+03	5.720E+03
7	5.720E+03	5.887E+03	5.721E+03	5.890E+03	8.045E+03	5.793E+03	5.720E+03	5.720E+03
8	5.720E+03	5.835E+03	5.760E+03	5.918E+03	7.983E+03	57.95.6435	5.830E+03	5.720E+03
9	5.720E+03	5.804E+03	5.720E+03	5.923E+03	8.186E+03	6.656E+03	6.412E+03	5.720E+03
10	5.720E+03	6.055E+03	5.720E+03	5.920E+03	6.413E+03	5.720E+03	5.744E+03	5.720E+03
Average	5.720E+03	5.817E+03	5.731E+03	5.930E+03	7.431E+03	6.101E+03	5.872E+03	**5.720E+03**
Std*	3.186E-01	1.025E+02	2.188E+01	4.940E+01	6.920E+02	3.869E+02	2.010E+02	**9.090E-13**
Best	5.720E+03	5.720E+03	5.720E+03	5.890E+03	6.162E+03	5.720E+03	5.720E+03	5.720E+03
Worst	5.721E+03	6.055E+03	5.786E+03	6.075E+03	8.186E+03	6.805E+03	6.412E+03	5.720E+03

* Standard deviation.

The boxplot representation is an efficient way to show the reliability of algorithms. Therefore, an explicit statistical embodiment of the convergence rate for all optimizers is plotted in Fig. 3. Each boxplot's lower and upper boundaries show the maximum and minimum values of objective function calculated over all runs for each algorithm, respectively. According to Fig. 4, the proposed kWOA generates more robust solutions in terms of the objective function's mean, minimum, and maximum values. Even though the performance is quite similar to the HHO algorithm on average, it is worth pointing out that the kWOA performs more robustly. Furthermore, it is clear that the HHO and ALO algorithms have demonstrated superior performance compared to other algorithms.

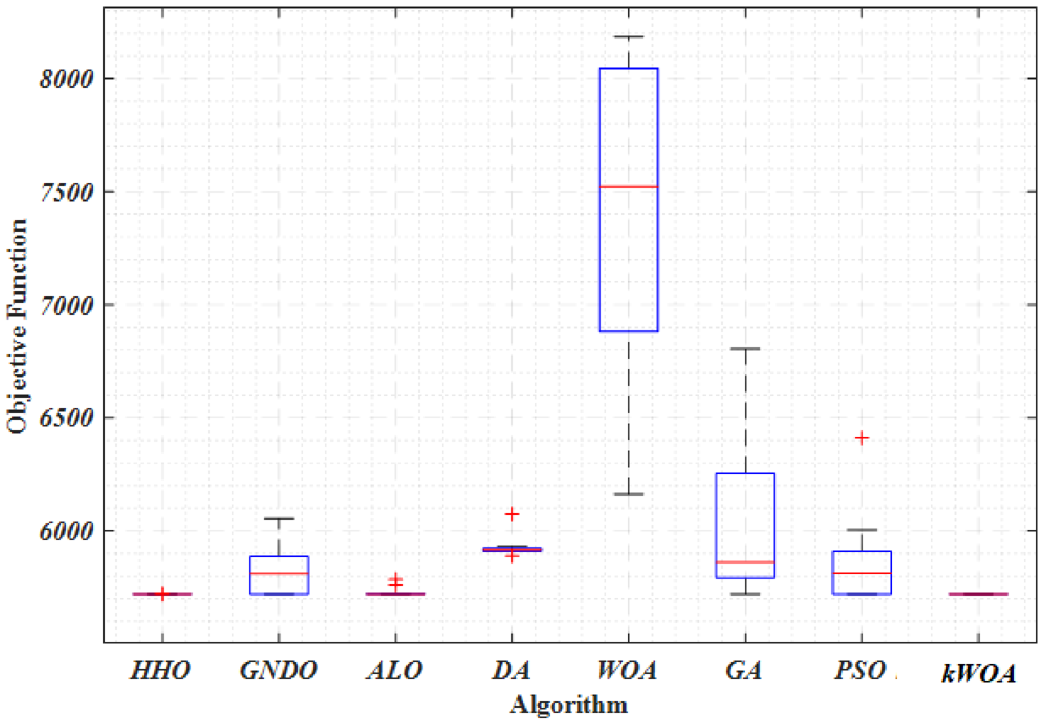

Fig. 4 Boxplots of obtained results by all mentioned algorithms for 10 runs.

To show the ability of algorithms to escape from falling into local optima, their convergence curves are plotted in Fig. 5. In this figure, it is seen that the k WOA was converged in iteration 52 for the best design. As is known, the reason why the starting points on the graphs in Fig. 5 are not the same is because a penalty approach based on equation (46) was used to avoid violating constraints. Therefore, all the solutions obtained in the initial iterations of the algorithm may be in the infeasible region, which caused the penalty function value to increase and become zero after the algorithm iterations [37].

$$f_p(x) = f(x) + \lambda \sum_{k=1}^{m} \delta_k [g_k(x)]^2 \tag{46}$$

where, f is the objective function, λ is the penalty coeficiente, m number of constraints, and δ_k is defined in equation (47) as an indicator of process violation:

$$\begin{Bmatrix} \delta_k = 1 \; if \; constraint \; g_k \; is \; violated \\ \delta_k = 0 \; if \; constraint \; g_k \; is \; satisfied \end{Bmatrix} \tag{47}$$

This part of the research aims to optimize the design variables of STHEs using metaheuristic techniques and the Bell-Delaware design method. Generally, optimizing these important STHE parameters can decrease the fixed cost and operating costs of STHE. Table 7 reports the best value of each parameter obtained from the optimization process by all algorithms. It is important to mention that all the obtained values of design variables satisfy the defined constraints. There are no major differences between the obtained values of variables.

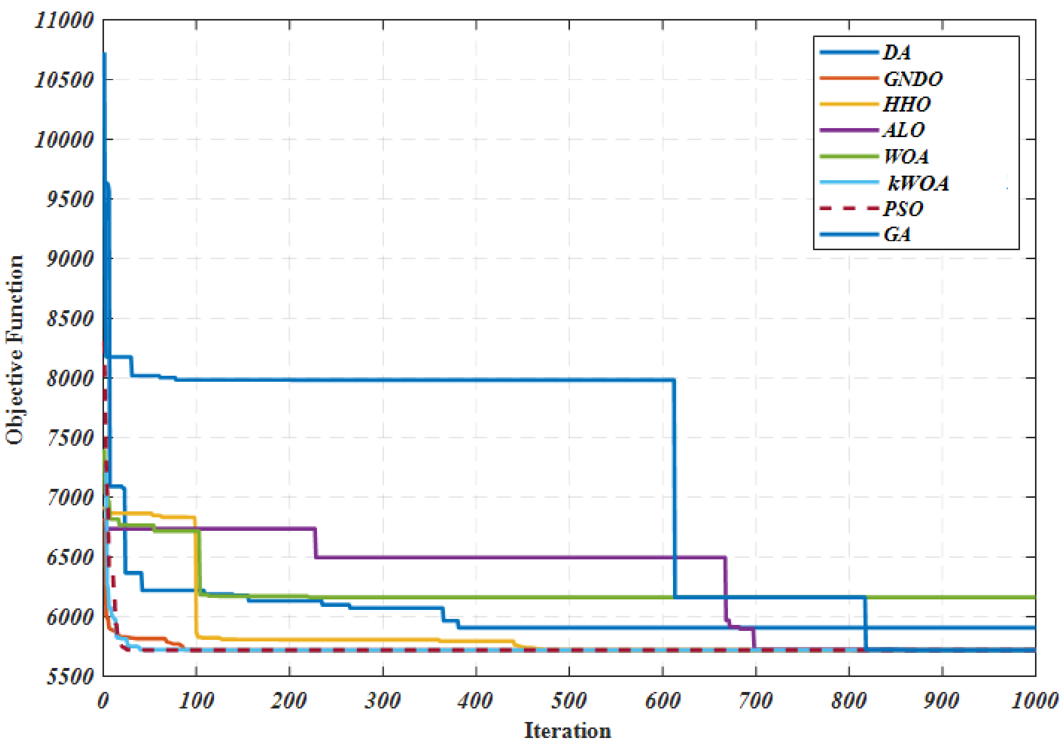

Fig. 5 Convergence curves of all mentioned algorithms for the best run.

Table 7. Values obtained for the design variables in the best run with the different optimizers.

	D_s (m)	d_o (m)	N_t --	A m^2	L m	P_t m	TL °	s -	L_{bc} m
HHO	3.00E-01	6.35E-03	9.48E+02	4.31E+01	2.28E+00	7.90E-03	9.00E+01	1.00E+00	1.17E-01
GNDO	3.00E-01	6.35E-03	9.48E+02	4.34E+01	2.29E+00	7.90E-03	9.00E+01	1.00E+00	1.23E-01
ALO	3.00E-01	6.35E-03	9.48E+02	4.34E+01	2.29E+00	7.90E-03	9.00E+01	1.00E+00	1.23E-01
DO	3.00E-01	6.35E-03	9.48E+02	4.34E+01	2.29E+00	7.90E-03	9.00E+01	1.00E+00	1.23E-01

WOA	3.20E-01	6.35E-03	1.08E+03	4.68E+01	2.17E+00	7.90E-03	9.00E+01	1.00E+00	1.54E-01
GA	3.00E-01	6.35E-03	9.48E+02	4.34E+01	2.29E+00	7.90E-03	9.00E+01	1.00E+00	1.23E-01
PSO	3.00E-01	6.35E-03	9.48E+02	4.34E+01	2.29E+00	7.90E-03	9.00E+01	1.00E+00	1.23E-01
kWOA	3.00E-01	6.35E-03	9.48E+02	4.34E+01	2.29E+00	7.90E-03	9.00E+01	1.00E+00	1.23E-01
	L_{boi}	B_c	L/D_s	ΔP_t	ΔP_s	C_{op}	C_{fix}	TAC	
	m	%		Pa	Pa	USD/year	USD/year	USD/year	
HHO	0.117	45	7.594E+00	1.356E+04	9.285E+03	6.649E+02	5.120E+03	5.785E+03	
GNDO	0.1968	45	7.645E+00	1.364E+04	5.064E+03	5.769E+02	5.143E+03	5.720E+03	
ALO	0.1968	45	7.645E+00	1.364E+04	5.064E+03	5.769E+02	5.143E+03	5.720E+03	
DO	0.1967	45	7.645E+00	1.363E+04	5.067E+03	5.770E+02	5.143E+03	5.720E+03	
WOA	0.1536	25	6.782E+00	1.369E+04	2.172E+04	5.419E+03	9.363E+02	6.356E+03	
GA	0.1968	45	7.645E+00	1.364E+04	5.064E+03	5.769E+02	5.143E+03	5.720E+03	
PSO	0.1968	45	7.645E+00	1.364E+04	5.064E+03	5.769E+02	5.143E+03	5.720E+03	
kWOA	0.197	45	7.645E+00	1.364E+04	5.064E+03	5.769E+02	5.143E+03	5.720E+03	

Consequently, the obtained designs show the efficiency of optimization algorithms in reducing the costs of the design and operation phases of STHEs. Table 7 shows that all the constraints of investigated case study are satisfied for all obtained designs.

4.3. Reliability-based design optimization of STHE

4.3.1. Validation the proposed RA model

To solve the RBDO problem of STHE design, we couple a surrogate-based Monte Carlo technique with kWOA in the design process. First, we investigate the efficiency of the adaptive surrogate model by solving five numerical reliability benchmark problems. Table 8 presents the details of mentioned benchmark problems.

As previously discussed, the primary goal of employing a surrogate model, the CVRBF method, in conjunction with a simulation-based technique such as MCS is to reduce the use of the STHE design model. This is achieved by creating an efficient surrogate model that accurately approximates the behavior of the STHE system with fewer simulations than direct methods. In the context of RBDO, this surrogate model enables rapid and less resource-intensive reliability assessments of the STHE design under uncertainty. By integrating the CVRBF model with MCS, we can quickly evaluate the surrogate model in each iteration of the optimization process, significantly cutting down on computational time.

The performance of the proposed CVRBF method in solving the numerical benchmark problems is compared to the MCS, first-order reliability method (FORM), importance sampling (IS), and first-order control variate method (FOCM) [51]. To calculate the relative error of the proposed CV and other techniques than to MCS, equation (48) was used [52].

$$\varepsilon = \frac{\left|P_f - P_f^{MCS}\right|}{P_f^{MCS}} \times 100 \tag{48}$$

where P_f and P_f^{MCS} indicate the failure probability calculated trough the under-study reliability analysis techniques and MCS.

Table 8. Selected benchmark reliability problems [51].

No.	Limit state function
1	$g(\boldsymbol{X}) = 1.1 - 0.00115x_1x_2 + 0.00157x_2^2 + 0.00117x_1^2 + 0.0135x_3x_2 - 0.0705x_2 - 0.00534x_1 - 0.0149x_1x_3 - 0.0611x_4x_2 + 0.0717x_1x_4 - 0.226x_3 + 0.0333x_3^2 - 0.558x_3x_4 + 0.998x_4 - 1.339x_4^2$ where: $x_1 = EX - II(10.0{,}5.0);\ x_2 = N(25.0{,}5.0);\ x_3 = N(0.8{,}0.2);\ x_1 = LN(6.25E-02{,}6.25E-02)$
2	$g(\boldsymbol{X}) = \frac{5}{2} + \frac{1}{216}(x_1 + x_2 - 20)^4 - \frac{33}{140}(x_1 + x_2)$ where: $x_1 = N(10.0{,}0.3);\ x_2 = N(10.0{,}0.3)$
3	$g(\boldsymbol{X}) = 2 - x_2 - 0.1x_1^2 + 0.06x_1^3$ where: $x_1 = U(0.0{,}1.0);\ x_2 = U(0.0{,}1.0)$
4	$g(\boldsymbol{X}) = -0.5(x_1 - x_2)^2 - \frac{x_1 - x_2}{\sqrt{2}} + 3$ where: $x_1 = U(0.0{,}1.0);\ x_2 = U(0.0{,}1.0)$
5	$g(\boldsymbol{X}) = \exp(0.2x_1 + 6.2) - \exp(0.47x_2 + 5.0)$ where: $x_1 = U(0.0{,}1.0);\ x_2 = U(0.0{,}1.0)$

U: uniform distribution; N: Normal distribution; LN: Log-normal distribution; EX-II: Extreme type II.

The reliability analysis of selected benchmarks used by the under-study reliability analysis techniques are summarized in Table 9. The failure probability of examples calculated through MCS are $P_f^{ex1} = 0.0823$, $P_f^{ex2} = 0.0029$, $P_f^{ex3} = 0.0344$, $P_f^{ex4} = 0.1056$, and $P_f^{ex5} = 0.0094$, respectively. Moreover, the failure probability's value of these examples is calculated using other methods (i.e., MCS, FORM, IS, and FOCM). Table 9 reports the details of the results of the examples in terms of the failure probability, computed relative error, and the number of limit state function evaluations.

Table 9. Results of reliability analysis of benchmark problems.

	MCS		FORM			IS			FOCM [62]			CVRBF		
No.	P_f^{MCS}	N_{eval}	P_f	N_{eval}	$\varepsilon(\%)$	P_f	N_{eval}	$\varepsilon(\%)$	P_f	N_{eval}	$\varepsilon(\%)$	P_f	N_{eval}	$\varepsilon(\%)$
1	0.0823	10^6	-	100	-	0.0968	9000	17.61	0.080	721	2.79	0.0951	100	15.55
2	0.0029	10^6	0.0062	100	10.3	0.0025	5000	13.79	0.0029	1082	0.00	0.0031	150	6.89
3	0.0344	10^6	0.0228	100	33.72	0.0375	4000	9.00	0.0359	351	4.36	0.0344	100	0.00
4	0.1056	10^6	0.0019	100	98.22	0.0918	2000	13.06	0.0985	536	6.72	0.1131	100	3.20
5	0.0094	10^6	0.0094	100	0.00	0.0084	1000	1.70	0.0094	110	0.00	0.0094	150	0.00

The analysis of the obtained results in Table 9 reveals that the FOCM method [51] has the least relative error than calculated results of MCS. Despite the robust results of this method compared to the under-study reliability analysis methods, it has a high computational time (the performance function evaluation number). On the other hand, the proposed CVRBF method has been able to accurately estimate the failure probability of all examples with a suitable number of performance function evaluations. In addition, the run time for a full reliability analysis (in seconds) of the proposed surrogate model for all examples is $t_{eval} = 110s$, $t_{eval} = 40s$, $t_{eval} = 95s$, $t_{eval} = 130s$, $t_{eval} = 50s$ respectively. It should be noted that we used a personal computer with 8 processing cores and 32 GB of RAM to perform the runs. Consequently, according to the observed results in Table 9, it can be claimed that the control variate-based surrogate model is extremely efficient and robust to reach the best result and is a great approach to evaluate the safety level of various structures/systems.

4.3.2. The performance of the proposed approach for an optimal design of STHE

The problem of STHE design is reformulated as a RBDO problem (Eq. 24). According to the carried-out study by Ref. [24], the inlet flow temperatures, the mass flow rates, and fouling resistance parameters were recognized as the most effective uncertainty parameters that effect on the performance of the system. Thus, these parameters were considered as the random variables in the RBDO process. Table 10 reports the information of random variables. To simulate the effect of uncertainty on the mentioned parameters, the samples were generated assuming the truncated normal distribution.

Table 10. The information of uncertain variables.

	Parameter	Distribution	Average	Variance
Tube	Mass flow rate ($\frac{kg}{s}$)	Truncated normal	22.7	0.227
	Inlet flow temperatures (℃)	Truncated normal	33.9	0.339
	Fouling resistance	Truncated normal	1.70E-04	1.70E-06
Shell	Inlet flow temperatures (℃)	Truncated normal	23.9	0.339
	Fouling resistance ($\frac{m^2k}{W}$)	Truncated normal	1.70E-04	1.70E-06

The penalty function approach is employed to handle constraints in the RBDO similarly to the DO processes. When the target failure probability is exceeded, a significant constant number is added to the objective function's value. This encourages the optimization algorithm, which aims to minimize the objective function, to find the optimal decision variable values that comply with the probabilistic constraints.

Finding the best values for setting parameters of the RBF neural network is one of the existing challenges for the use of these methods. These parameters include the weights between the hidden and output layers, the activation function, and the number of neurons in the hidden layer. To achieve an efficient RBF model in forecasting the limit state function of the RBDO process to a high level of accuracy, the hybrid kWOA was used to optimize the parameters of RBF in the training phase. Noticeably, the Gaussian function was used as the radial function here. Table 11 presents the values of MAPE and SD for the performance level achieved by CVRBF in the training phase. It is clear that the performance generality results of the hybrid WOA-based CVRBF are acceptable, and they can be incorporated into the RBDO procedure to estimate the required system responses.

Table 11. Performance of surrogate model for predicting the response of system.

Model	**MAPE**	**SD**

CVRBF	2.61	2.01

In the RBDO process, the probabilistic constraint was defined as the safety level of the STHE optimization problem with 1% and 5% failure probability. Moreover, the number of search agents and the maximum number of iterations for k-means-based WOA were 50 and 100, respectively.

Upon evaluating the probabilistic design problem under *scenarios 1* (target failure probability, $\mathrm{P_f^t} = 1\%$) and 2 ($\mathrm{P_f^t} = 5\%$), we obtained final objective function values of 12,172.61 USD/year and 10,393.15 USD/year, respectively. These results demonstrate that our model achieved the minimum cost values while satisfying the reliability constraints of 99% and 95% for *scenarios 1* and *2*, respectively.

Our RBDO framework addresses the inherent trade-off between reducing failure probability and increasing design costs by optimizing the STHE design to meet specific reliability constraints under uncertainty. As the target reliability level is raised, the design becomes more robust, which naturally leads to higher costs. For instance, in Scenario 1, where the target failure probability is set to 1%, the optimized design cost escalated to 12,172.61 USD/year, marking a substantial increase from the deterministic optimization (DO) cost of 5,719.74 USD/year. Similarly, in Scenario 2, with a target failure probability of 5%, the design cost rose to 10,393.15 USD/year.

Figure 5 shows the convergence curves for the best run of our RBDO model under both scenarios. The model converged at iteration 58 for scenario 1 and at iteration 9 for scenario 2. The later convergence in scenario 1 can be attributed to the higher complexity of its probability constraint ($Reliability_{system} \geq Reliability_{target} = 99\%$). Generally, achieving higher levels of reliability in design problems often leads to increased costs, making it challenging to balance design expenses with system safety.

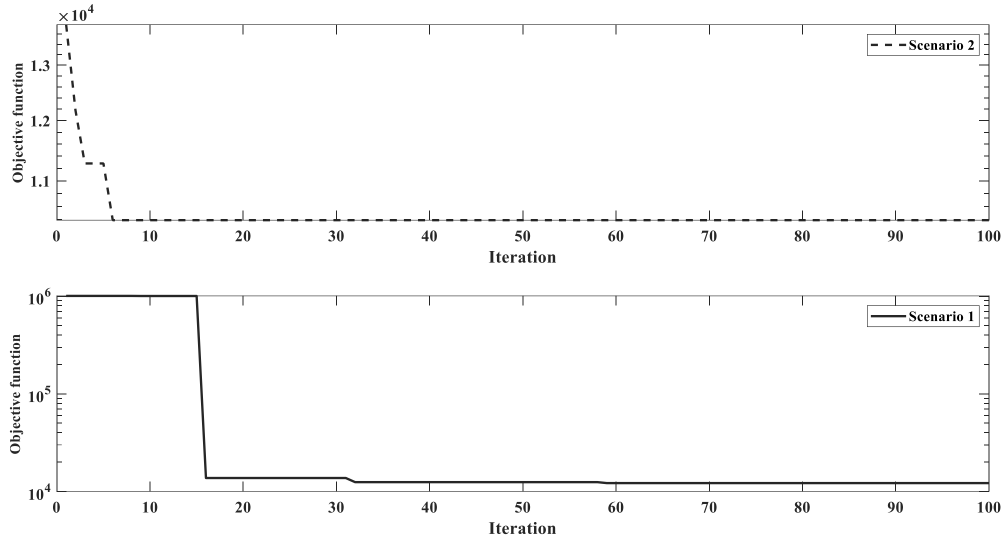

Fig. 6. Convergence curves of two RBDO scenarios.

Furthermore, a comparative analysis of RBDO and DO designs is presented in Table 12. The presented results in Table 12 show that the value of the objective function increased up to 112% and 82% for two *scenarios 1* and *2*, respectively. In order to control the feasibility of the safe design found by the RBDO process, the histograms of constraints are plotted in Fig. 7. In this figure, dashed red lines indicate the safe regions of the constraints. These regions show the areas where the constraints are satisfied and the design is considered feasible. The permissible bounds for each constraint, which define the allowable range of values for the corresponding design parameter, are described in Section 2. The histograms demonstrate the effectiveness of the RBDO approach in maintaining the system's safety level under uncertain conditions that may occur during its service life.

Table 12. Comparison of DO and RBDO proposed approaches.

Approach	Cost ($/year)	Reliability (%)
DO	5719.74	12
$RBDO_1$	12172.61	99
$RBDO_2$	10393.15	95

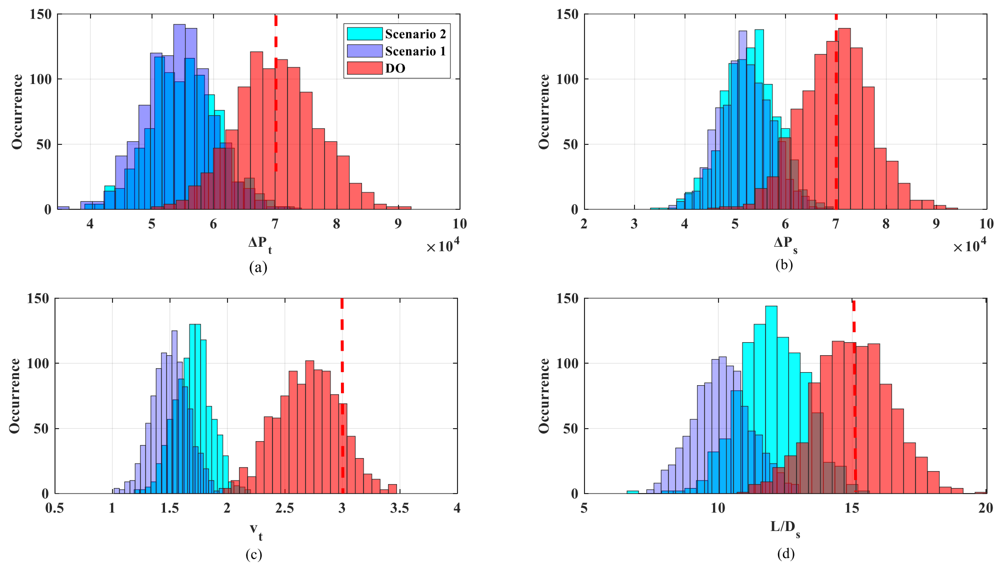

Fig. 7. The frequency of constraints for the DO and RBDO designs.

4.4. Discussion

In the sub-sections 4.2 and 4.3, the proposed kWOA algorithm was displayed to outperform the other algorithms (i.e., the PSO, GA, HHO, GNDO, and ALO) and its original WOA algorithm under two phases: (1) CEC'2020 test function, and (2) optimization of SHTEs. The search algorithms' starting point significantly impacts the convergence and effectiveness of the search in the problem space. In this study, the use of the k-means clustering approach in the first stage of the WOA, i.e., the generation of initial population, increased the probability of achieving the global optimal solution and expedited the convergence process. The results showed that the proposed algorithm was able to effectively solve the mathematical benchmark functions and complex optimization problems of heat exchangers. Additionally, in section 4.3, its integration with an alternative approach for optimal design of heat exchangers under uncertainty and the constraint of failure probability was confirmed, demonstrating the ability to provide a robust design.

Finally, it is necessary to state the possible limitations of this study. While using new approaches to improve the performance of optimization algorithms and solve complex RBDO problems with surrogate models can enhance the speed of algorithm convergence and computation time, it may also reduce the modeling accuracy in a complex system with a large number of random variables. To address this issue, using new reliability methods (i.e., Bayesian active learning [53], Parallel adaptive Bayesian quadrature [54], Enhanced Hamiltonian-MCS [55], and adaptive Kriging-probability density evolution method [56].) in conjunction with the proposed kWOA algorithm may be a good suggestion. Moreover, it is recommend that a risk-based study conduct with considering the cost of failure to make a comparison fair between the deterministic and probabilistic approaches. To this end, the introduced approach in [57] can be used.

Furthermore, despite the excellent performance of the proposed approach in solving the problem of STHEs, it is worth noting that, according to the No Free Lunch (NFL) theorem, this approach may not be suitable for solving all complex engineering problems [58].

5. Conclusions

This study introduces a novel hybrid approach for optimizing the design of STHE using a RBDO method. The approach combines a control CVRBF and MCS to estimate the system response of the STHE during the design process. We enhanced the WOA by integrating the k-means clustering method to increase the efficiency of the optimization process. Our results indicate that the improved WOA algorithm is an effective deterministic optimization approach for designing the optimal layout of the STHE, outperforming other meta-heuristic algorithms used for the same purpose.

In the RBDO section, we employed a surrogate approach based on the CVRBF method to reduce computational costs. We first demonstrated the efficacy of the surrogate model in solving five benchmark reliability problems, showcasing its robustness in evaluating complex problems with non-explicit limit state functions. We then applied the model to solve the RBDO problem of STHEs. The results revealed that the proposed RBDO framework, which combines CVRBF, MCS, and k-means-based WOA, is the most effective approach for achieving a safe design of the STHEs. It introduces the concept of designing under uncertainty in this field and significantly reduces the failure probability of the design under uncertainty. In our case study, under two scenarios, the failure probability decreased from 89% to 1% and 5%, respectively. However, this decrease was accompanied by an increase in design costs of 112% and 82% for the two scenarios considered.

The comparison of the final design obtained from the proposed method with the best deterministic approach design demonstrates the superiority of the proposed RBDO framework in increasing the reliability of the design under uncertainty. In summary, the proposed framework provides a robust approach to designing important equipment in the field of process engineering. Future research can further enhance this approach by incorporating a reliability-based multi-objective optimization framework, which can be applied to the STHE.

Our proposed k-means-based kWOA and CVRBF approach for RBDO have demonstrated effectiveness in optimizing STHEs. However, their applicability may be limited by the computational complexity of kWOA for large-scale problems and the sensitivity of both methods to parameter selection. Additionally, the accuracy of the probabilistic models used to represent uncertainties in RBDO could impact the reliability of the optimized designs. While our methods have shown promise in the specific context of STHEs, further research is needed to evaluate their generalizability and effectiveness across different engineering problems and to address these potential limitations.

Data Availability The data presented in this study are available on request from the corresponding author.

[1] R.K. Sinnott, Heat-transfer Equipment, in: Chemical Engineering Design, 4th ed., Butterworth-Heinemann, 2005: p. 1056.

[2] R.K. Shah, D.P. Sekulic, Fundamentals of Heat Exchanger Design, John Wiley & Sons, Ltd, 2003. https://doi.org/10.1002/9780470172605.ch9.

[3] A.C. Caputo, A. Federici, P.M. Pelagagge, P. Salini, On the selection of design methodology for shell-and-tube heat exchangers optimization problems, Thermal Science and Engineering Progress 34 (2022) 101384. https://doi.org/10.1016/j.tsep.2022.101384.

[4] F.T. Mizutani, F.L.P. Pessoa, E.M. Queiroz, S. Hauan, I.E. Grossmann, Mathematical programming model for heat-exchanger network synthesis including detailed heat-exchanger designs. 1. Shell-and-tube heat-exchanger design, Industrial and Engineering Chemistry Research 42 (2003) 4009–4018. https://doi.org/10.1021/ie020964u.

[5] J.M. Ponce, M. Serna, V. Rico, A. Jiménez, Optimal design of shell-and-tube heat exchangers using genetic algorithms, in: 16th European Symposium on Computer Aided Process Engineering and 9th International Symposium on Process Systems Engineering, Elsevier, 2006: pp. 985–990. https://doi.org/10.1016/s1570-7946(06)80174-4.

[6] V.C. Onishi, M.A.S.S. Ravagnani, J.A. Caballero, Mathematical programming model for heat exchanger design through optimization of partial objectives, Energy Conversion and Management 74 (2013) 60–69. https://doi.org/10.1016/j.enconman.2013.05.011.

[7] X.-S. Yang, Nature-Inspired Algorithms and Applied Optimization, in: X.-S. Yang (Ed.), Springer International Publishing, 2018: pp. 1–26. https://doi.org/10.1007/978-3-319-67669-2.

[8] X.-S. Yang, S. Deb, S. Fong, Metaheuristic Algorithms: Optimal Balance of Intensification and Diversification, Applied Mathematics & Information Sciences 8 (2014) 977–983. https://doi.org/10.12785/amis/080306.

[9] P. Agrawal, H.F. Abutarboush, T. Ganesh, A.W. Mohamed, Metaheuristic Algorithms on Feature Selection: A Survey of One Decade of Research (2009-2019), IEEE Access 9 (2021) 26766–26791. https://doi.org/10.1109/ACCESS.2021.3056407.

[10] H. Sadeghzadeh, M.A. Ehyaei, M.A. Rosen, Techno-economic optimization of a shell and tube heat exchanger by genetic and particle swarm algorithms, Energy Conversion and Management 93 (2015) 84–91. https://doi.org/10.1016/j.enconman.2015.01.007.

[11] R. Selbaş, Ö. Kızılkan, M. Reppich, A new design approach for shell-and-tube heat exchangers using genetic algorithms from economic point of view, Chem. Eng. Process. Process Intensif. 45 (2006) 268–275. https://doi.org/10.1016/j.cep.2005.07.004.

[12] P. Wildi-Tremblay, L. Gosselin, Minimizing shell-and-tube heat exchanger cost with genetic algorithms and considering maintenance, International Journal of Energy Research 31 (2007) 867–885. https://doi.org/10.1002/er.1272.

[13] B.V. Babu, S.A. Munawar, Differential evolution strategies for optimal design of shell-and-tube heat exchangers, Chemical Engineering Science (2007). https://doi.org/10.1016/j.ces.2007.03.039.

[14] E.H. de V. Segundo, A.L. Amoroso, V.C. Mariani, L. dos S. Coelho, Economic optimization design for shell-and-tube heat exchangers by a Tsallis differential evolution, Appl. Therm. Eng. 111 (2017) 143–151. https://doi.org/10.1016/j.applthermaleng.2016.09.032.

[15] D.K. Mohanty, Gravitational search algorithm for economic optimization design of a shell and tube heat exchanger, Applied Thermal Engineering (2016). https://doi.org/10.1016/j.applthermaleng.2016.06.133.

[16] C.A.R. do Nascimento, V.C. Mariani, L. dos S. Coelho, Integrative numerical modeling and thermodynamic optimal design of counter-flow plate-fin heat exchanger applying neural networks, International Journal of Heat and Mass Transfer 159 (2020) 120097. https://doi.org/10.1016/j.ijheatmasstransfer.2020.120097.

[17] A.B. Colaço, V.C. Mariani, M.R. Salem, L. dos S. Coelho, Maximizing the thermal performance index applying evolutionary multi-objective optimization approaches for double pipe heat exchanger, Applied Thermal Engineering 211 (2022) 118504. https://doi.org/10.1016/j.applthermaleng.2022.118504.

[18] M.H. Hamed, A.N. Shmroukh, M. Attalla, H.M. Maghrabie, Optimization of inserted coiled tube three-fluid heat exchanger using genetic algorithms, Engineering Applications of Artificial Intelligence 126 (2023) 106909. https://doi.org/10.1016/j.engappai.2023.106909.

[19] O.D. Lara-Montaño, F.I. Gómez-Castro, Optimization of a shell-and-tube heat exchanger using the grey wolf algorithm, in: Computer Aided Chemical Engineering, Elsevier, 2019: pp. 571–576. https://doi.org/10.1016/b978-0-12-818634-3.50096-5.

[20] H. Hajabdollahi, P. Ahmadi, I. Dincer, Exergetic optimization of shell-and-tube heat exchangers using NSGA-II, Heat Transfer Engineering 33 (2012) 618–628. https://doi.org/10.1080/01457632.2012.630266.

[21] O.D. Lara Montaño, F.I. Gómez Castro, C. Gutiérrez Antonio, Comparison of the performance of different metaheuristic methods for the optimization of shell-and-tube heat exchangers, Computers & Chemical Engineering 152 (2021) 107403. https://doi.org/10.1016/j.compchemeng.2021.107403.

[22] A. Şencan Şahin, B. Kiliç, U. Kiliç, Design and economic optimization of shell and tube heat exchangers using Artificial Bee Colony (ABC) algorithm, Energy Conversion and Management 52 (2011) 3356–3362. https://doi.org/10.1016/j.enconman.2011.07.003.

[23] M. Asadi, Y. Song, B. Sunden, G. Xie, Economic optimization design of shell-and-tube heat exchangers by a cuckoo-search-algorithm, Applied Thermal Engineering 73 (2014) 1032–1040. https://doi.org/10.1016/j.applthermaleng.2014.08.061.

[24] H. Azarkish, M. Rashki, Reliability and reliability-based sensitivity analysis of shell and tube heat exchangers using Monte Carlo Simulation, Applied Thermal Engineering 159 (2019) 113842. https://doi.org/10.1016/j.applthermaleng.2019.113842.

[25] W.H. Saldanha, F.R.P. Arrieta, P.I. Ekel, T.M. Machado-Coelho, G.L. Soares, Multi-criteria decision-making under uncertainty conditions of a shell-and-tube heat exchanger, International Journal of Heat and Mass Transfer 155 (2020) 119716. https://doi.org/10.1016/j.ijheatmasstransfer.2020.119716.

[26] S. Ohadi, J. Jafari-Asl, O.D.L. Montaño, N.S. Hamzehkolaei, Multi-Objective Reliability-Based Design Optimization of Shell-and-Tube Heat Exchangers Using Combined Subset Simulation Method and Naive Bayes Algorithm, in: Handbook of Smart Energy Systems, Springer International Publishing, 2022: pp. 1–18. https://doi.org/10.1007/978-3-030-72322-4_96-1.

[27] S. Mirjalili, A. Lewis, The Whale Optimization Algorithm, Advances in Engineering Software 95 (2016) 51–67. https://doi.org/10.1016/j.advengsoft.2016.01.008.

[28] M.M. Mafarja, S. Mirjalili, Hybrid Whale Optimization Algorithm with simulated annealing for feature selection, Neurocomputing 260 (2017) 302–312. https://doi.org/10.1016/j.neucom.2017.04.053.

[29] W. Guo, T. Liu, F. Dai, P. Xu, An improved whale optimization algorithm for forecasting water resources demand, Applied Soft Computing 86 (2020) 105925. https://doi.org/10.1016/j.asoc.2019.105925.

[30] X. Zhang, S. Wen, Hybrid whale optimization algorithm with gathering strategies for high-dimensional problems, Expert Systems with Applications 179 (2021) 115032. https://doi.org/10.1016/j.eswa.2021.115032.

[31] M.H. Nadimi-Shahraki, H. Zamani, S. Mirjalili, Enhanced whale optimization algorithm for medical feature selection: A COVID-19 case study, Computers in Biology and Medicine 148 (2022) 105858. https://doi.org/10.1016/j.compbiomed.2022.105858.

[32] D. Xiong, W. Fu, K. Wang, P. Fang, T. Chen, F. Zou, A blended approach incorporating TVFEMD, PSR, NNCT-based multi-model fusion and hierarchy-based merged optimization algorithm for multi-step wind speed prediction, Energy Conversion and Management 230 (2021) 113680. https://doi.org/10.1016/j.enconman.2020.113680.

[33] L. Peng, C. He, A.A. Heidari, Q. Zhang, H. Chen, G. Liang, N.O. Aljehane, R.F. Mansour, Information sharing search boosted whale optimizer with Nelder-Mead simplex for parameter estimation of photovoltaic models, Energy Conversion and Management 270 (2022) 116246. https://doi.org/10.1016/j.enconman.2022.116246.

[34] G. Hou, L. Gong, Z. Yang, J. Zhang, Multi-objective economic model predictive control for gas turbine system based on quantum simultaneous whale optimization algorithm, Energy Conversion and Management 207 (2020) 112498. https://doi.org/10.1016/j.enconman.2020.112498.

[35] J. MACQUEEN, SOME METHODS FOR CLASSIFICATION AND ANALYSIS OF MULTIVARIATE OBSERVATIONS, in: 1967: pp. 281–297.

[36] H.M. Mohammed, Z.Kh. Abdul, T.A. Rashid, A. Alsadoon, N. Bacanin, A new K-means grey wolf algorithm for engineering problems, WJE 18 (2021) 630–638. https://doi.org/10.1108/WJE-10-2020-0527.

[37] J. Jafari-Asl, M.E.A. Ben Seghier, S. Ohadi, P. Van Gelder, Efficient method using Whale Optimization Algorithm for reliability-based design optimization of labyrinth spillway, Applied Soft Computing 101 (2021) 107036. https://doi.org/10.1016/j.asoc.2020.107036.

[38] S.H. Mai, M.E.A. Ben Seghier, P.L. Nguyen, J. Jafari-Asl, D.-K. Thai, A hybrid model for predicting the axial compression capacity of square concrete-filled steel tubular columns, Engineering with

Computers 38 (2022) 1205–1222. https://doi.org/10.1007/s00366-020-01104-w.

[39] M. Rahmanshahi, J. Jafari-Asl, M. Shafai Bejestan, S. Mirjalili, A Hybrid Model for Predicting the Energy Dissipation on the Block Ramp Hydraulic Structures, Water Resour Manage 37 (2023) 3187–3209. https://doi.org/10.1007/s11269-023-03497-x.

[40] S. Gholizadeh, M. Mohammadi, Reliability-Based Seismic Optimization of Steel Frames by Metaheuristics and Neural Networks, ASCE-ASME J. Risk Uncertainty Eng. Syst., Part A: Civ. Eng. 3 (2017) 04016013. https://doi.org/10.1061/AJRUA6.0000892.

[41] M. Rashki, H. Azarkish, M. Rostamian, A. Bahrpeyma, Classification correction of polynomial response surface methods for accurate reliability estimation, Structural Safety 81 (2019) 101869. https://doi.org/10.1016/j.strusafe.2019.101869.

[42] M. Rashki, Hybrid control variates-based simulation method for structural reliability analysis of some problems with low failure probability, Applied Mathematical Modelling 60 (2018) 220–234. https://doi.org/10.1016/j.apm.2018.03.009.

[43] E.H. Houssein, E. Çelik, M.A. Mahdy, R.M. Ghoniem, Self-adaptive Equilibrium Optimizer for solving global, combinatorial, engineering, and Multi-Objective problems, Expert Systems with Applications 195 (2022) 116552. https://doi.org/10.1016/j.eswa.2022.116552.

[44] A.A. Heidari, S. Mirjalili, H. Faris, I. Aljarah, M. Mafarja, H. Chen, Harris hawks optimization: Algorithm and applications, Future Generation Computer Systems 97 (2019) 849–872. https://doi.org/10.1016/j.future.2019.02.028.

[45] Y. Zhang, Z. Jin, S. Mirjalili, Generalized normal distribution optimization and its applications in parameter extraction of photovoltaic models, Energy Conversion and Management 224 (2020) 113301. https://doi.org/10.1016/j.enconman.2020.113301.

[46] S. Mirjalili, The Ant Lion Optimizer, Advances in Engineering Software 83 (2015) 80–98. https://doi.org/10.1016/j.advengsoft.2015.01.010.

[47] Y. Meraihi, A. Ramdane-Cherif, D. Acheli, M. Mahseur, Dragonfly algorithm: a comprehensive review and applications, Neural Comput & Applic 32 (2020) 16625–16646. https://doi.org/10.1007/s00521-020-04866-y.

[48] J.H. Holland, Adaptation in natural and artificial systems : an introductory analysis with applications to biology, control, and artificial intelligence, First, MIT Press, Cambridge, Mass, 1992.

[49] J. Kennedy, R. Eberhart, Particle swarm optimization, in: Proceedings of ICNN'95 - International Conference on Neural Networks, Institute of Electrical and Electronics Engineers Available from IEEE Service Center, New York Piscataway, NJ, 1995: pp. 1942–1948. https://doi.org/10.1109/ICNN.1995.488968.

[50] A. Arcuri, G. Fraser, Parameter tuning or default values? An empirical investigation in search-based software engineering, Empir Software Eng 18 (2013) 594–623. https://doi.org/10.1007/s10664-013-9249-9.

[51] M. Ghalehnovi, M. Rashki, A. Ameryan, First order control variates algorithm for reliability analysis of engineering structures, Applied Mathematical Modelling 77 (2020) 829–847. https://doi.org/10.1016/j.apm.2019.07.049.

[52] J. Jafari-Asl, M.E.A. Ben Seghier, S. Ohadi, Y. Dong, V. Plevris, A Comparative Study on the Efficiency of Reliability Methods for the Probabilistic Analysis of Local Scour at a Bridge Pier in Clay-Sand-Mixed Sediments, Modelling 2 (2021) 63–77. https://doi.org/10.3390/modelling2010004.

[53] C. Dang, M.A. Valdebenito, M.G.R. Faes, J. Song, P. Wei, M. Beer, Structural reliability analysis by line sampling: A Bayesian active learning treatment, Structural Safety 104 (2023) 102351. https://doi.org/10.1016/j.strusafe.2023.102351.

[54] C. Dang, P. Wei, M.G.R. Faes, M.A. Valdebenito, M. Beer, Parallel adaptive Bayesian quadrature for rare event estimation, Reliability Engineering & System Safety 225 (2022) 108621. https://doi.org/10.1016/j.ress.2022.108621.

[55] D. Thaler, S.L.N. Dhulipala, F. Bamer, B. Markert, M.D. Shields, Enhanced Hamiltonian Monte Carlo simulations using Hamiltonian neural networks, Proc Appl Math and Mech 22 (2023) e202200188. https://doi.org/10.1002/pamm.202200188.

[56] T. Zhou, S. Marelli, B. Sudret, Y. Peng, AK-PDEMi: A failure-informed enrichment algorithm for improving the AK-PDEM in reliability analysis, Mechanical Systems and Signal Processing 180 (2022) 109435. https://doi.org/10.1016/j.ymssp.2022.109435.

[57] A.T. Beck, W.J.D.S. Gomes, A comparison of deterministic, reliability-based and risk-based structural optimization under uncertainty, Probabilistic Engineering Mechanics 28 (2012) 18–29. https://doi.org/10.1016/j.probengmech.2011.08.007.

[58] M. Rashki, M.G.R. Faes, No-Free-Lunch Theorems for Reliability Analysis, ASCE-ASME J. Risk Uncertainty Eng. Syst., Part A: Civ. Eng. 9 (2023) 04023019. https://doi.org/10.1061/AJRUA6.RUENG-1015.